Short Article

Cell Host & Microbe

Quorum Sensing Attenuates Virulence in *Sodalis praecaptivus*

Graphical Abstract

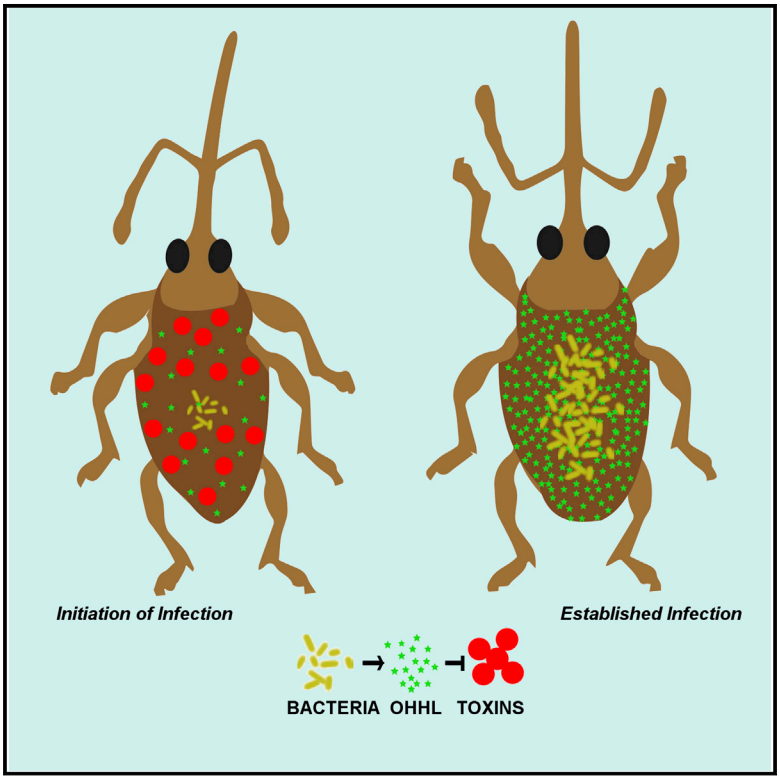

Authors

Shinichiro Enomoto, Abhishek Chari, Adam Larsen Clayton, Colin Dale

Correspondence

colin.dale@utah.edu

In Brief

Enomoto et al. show that a progenitor of the widely distributed *Sodalis*-allied insect endosymbionts utilizes quorum sensing to suppress virulence factors following the establishment of infection. This allows bacteria to maintain a benign and persistent infection in their insect host, possibly facilitating the evolution of mutualistic relationships.

Highlights

- Quorum sensing negatively regulates virulence in *Sodalis praecaptivus*
- Mutant strains defective in quorum sensing have an insect-killing phenotype
- Killing occurs as a result of the production of insecticidal toxins
- Limiting bacterial toxin production may facilitate a stable and benign infection

Enomoto et al., 2017, Cell Host & Microbe *21*, 629–636
May 10, 2017 Published by Elsevier Inc.
http://dx.doi.org/10.1016/j.chom.2017.04.003

Cell Host & Microbe
Short Article

Quorum Sensing Attenuates Virulence in *Sodalis praecaptivus*

Shinichiro Enomoto,[1] Abhishek Chari,[1] Adam Larsen Clayton,[1] and Colin Dale[1,2,*]
[1]Department of Biology, University of Utah, 257 South 1400 East, Salt Lake City, UT 84112, USA
[2]Lead Contact
*Correspondence: colin.dale@utah.edu
http://dx.doi.org/10.1016/j.chom.2017.04.003

SUMMARY

Sodalis praecaptivus **is a close relative and putative environmental progenitor of the widely distributed, insect-associated, *Sodalis*-allied symbionts. Here we show that mutant strains of *S. praecaptivus* that lack genetic components of a quorum-sensing (QS) apparatus have a rapid and potent killing phenotype following microinjection into an insect host. Transcriptomic and genetic analyses indicate that insect killing occurs as a consequence of virulence factors, including insecticidal toxins and enzymes that degrade the insect integument, which are normally repressed by QS at high infection densities. This method of regulation suggests that virulence factors are only utilized in early infection to initiate the insect-bacterial association. Once bacteria reach sufficient density in host tissues, the QS circuit represses expression of these harmful genes, facilitating a long-lasting and benign association. We discuss the implications of the functionality of this QS system in the context of establishment and evolution of mutualistic relationships involving these bacteria.**

INTRODUCTION

Many eukaryotes harbor mutualistic bacteria that increase host fitness and facilitate environmental niche diversification (Douglas, 2014). Insects serve as useful systems for the study of symbiosis because they are readily amenable to genomic and experimental study. While much is known about the evolution and functions of symbiosis in insects (Moran et al., 2008), little is known about how these mutualistic associations originate. One conspicuous finding is that certain bacterial phylotypes are predisposed to the development of these mutualisms. Examples include representatives of the *Sodalis* genera, which are found in a wide range of distantly related insect hosts (Snyder et al., 2011; Clayton et al., 2012).

Although certain symbionts provide specialized functions for their insect hosts (e.g., defense: Oliver et al., 2010), many just provide simple nutritional supplements, such as amino acids and vitamins (Douglas, 2009). Since these metabolites can be made by a wide range of bacteria, the notion of specialized function cannot explain the propensity of certain phylotypes to develop these associations. Rather, selected lineages seem predisposed to developing these associations as a result of genetic adaptations (Sachs et al., 2013). One of the most significant challenges in host association involves circumventing the sophisticated physical and molecular defenses that prevent bacterial entry and colonization. To this end, pathogens have evolved numerous molecular adaptations (virulence properties) to combat these processes and enhance bacterial infection. These range from relatively innocuous physical adaptations that facilitate resistance to factors of immunity to the secretion of enzymes and toxins that degrade host integument and inflict damage on tissues and cells (Vallet-Gely et al., 2008). It stands to reason that mutualists would experience stronger selection to limit the application of virulence in order to maximize host fitness and the likelihood of success of the resulting association.

In this study, we explore interactions between a close free-living relative of the *Sodalis*-allied insect endosymbionts, *Sodalis praecaptivus* (Clayton et al., 2012), and a grain weevil host, *Sitophilus zeamais*, that harbors a very recently derived *Sodalis*-allied endosymbiont (Lefèvre et al., 2004). Close relatives of *S. praecaptivus* have been identified in a wide range of insect hosts (Snyder et al., 2011; Clayton et al., 2012), and genomic analyses indicate that these mutualistic symbionts have evolved repeatedly and independently from an *S. praecaptivus*-like antecedent, undergoing substantial genome degeneration and size reduction as a consequence of the loss of many genes that lack adaptive value following the transition to the static symbiotic lifestyle (Clayton et al., 2012; Husnik and McCutcheon, 2016). Regarding their origin, the closest relatives of *S. praecaptivus* have been found in certain stinkbugs and chestnut weevils, in which these bacteria have a sporadic frequency of infection among insect populations (Kaiwa et al., 2010; Toju and Fukatsu, 2011), suggesting that they are not maternally transmitted by these insects but are instead acquired horizontally from the environment by each new insect generation. Since such a transient association is not compatible with the notion of obligate mutualism, we proposed that these insects may serve as vectors for the transmission of these bacteria to alternative hosts; namely the trees that the stinkbugs are known to feed upon (Clayton et al., 2012). In support of this, *S. praecaptivus* shares many genetic features (including genes encoding plant virulence factors) with the closely related phytopathogenic lineage comprising *Erwinia* and relatives, which are also often vectored by insects (Nadarasah and Stavrinides, 2011).

The regulation of gene expression is an important adaptive trait that facilitates the modification of physiology in accordance with the environment. One such mode of regulation is quorum

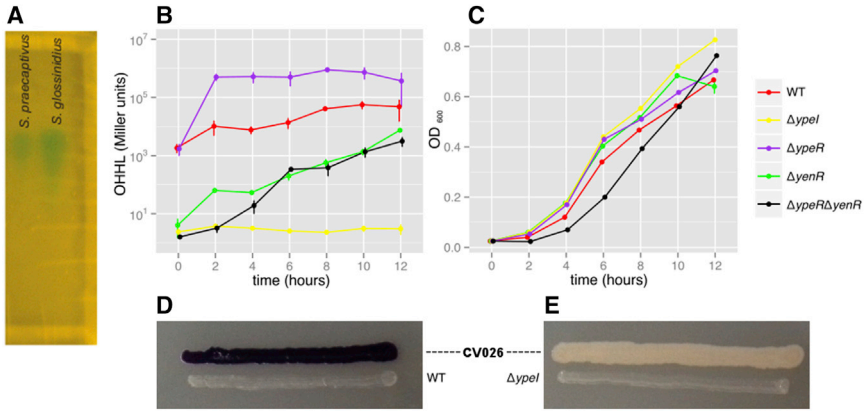

Figure 1. Characterization of the *S. praecaptivus* QS System

(A) TLC plate with ethyl acetate extracts derived from culture supernatants of *S. praecaptivus* and *S. glossinidius*. The plate was overlaid with an *A. tumefaciens* N-acyl homoserine lactone (AHL) reporter strain that produces blue spots in the presence of AHL molecules. This assay shows that *S. praecaptivus* and *S. glossinidius* each produce a single AHL molecule, which was previously characterized by mass spectrometry as OHHL in *S. glossinidius*.

(B and C) OHHL production (assayed using the *A. tumefaciens* reporter strain) (B) and growth (OD_{600}) (C) of WT and mutant strains of *S. praecaptivus*. Data were obtained from three biological replicates, and error bars show standard errors.

(D and E) Plate-based assays of AHL production from the *S. praecaptivus* WT (D) and Δ*ypeI* (E) strains (respectively) using the *Chromobacterium violaceum* CV026 reporter strain, which produces a violet pigment in the presence of AHLs.

sensing (QS), in which bacteria synthesize an autoinducer pheromone that increases in accordance with bacterial density and interacts at a threshold concentration with response regulators to facilitate changes in gene expression (Fuqua et al., 2001; Waters and Bassler, 2005). In the current study, we investigated the role of a QS system in *S. praecaptivus* and found that it negatively regulates a potent insect-killing phenotype. We propose that the negative regulation of virulence by QS is an important adaptation that contributes to the ability of *Sodalis*-allied symbionts to develop and sustain associations with insects.

RESULTS

S. praecaptivus and *S. glossinidius* Maintain Homologous Quorum-Sensing Systems

The tsetse fly symbiont *S. glossinidius* was previously shown to produce N-(3-oxohexanoyl) homoserine lactone (OHHL) as a QS signaling molecule via the protein product of a gene designated *sogI* (Pontes et al., 2008). To characterize the *S. praecaptivus* signaling molecule, we separated ethyl acetate extracts of *S. glossinidius* and *S. praecaptivus* culture media by thin-layer chromatography (TLC) and overlaid them with an *Agrobacterium tumefaciens* reporter strain that yields a blue spot in the presence of an N-acyl homoserine lactone (Zhu et al., 2003). Since the resulting spots co-localized on the TLC plate, we conclude that *S. praecaptivus* also produces OHHL (Figure 1A). In addition, *S. praecaptivus* maintains two LuxR-like response regulators (*ypeR* and *yenR*; locus tags Sant_3587 and Sant_1175, respectively) sharing >90% amino acid sequence identity with orthologs from *S. glossinidius*.

Transcriptomic Analysis of the *S. praecaptivus* QS System

To identify genes regulated by quorum sensing, we used RNA sequencing (RNA-seq) to compare gene expression levels in a Δ*ypeI* mutant strain of *S. praecaptivus* in vitro in the presence or absence of 10 μg/mL OHHL, which mimics a high cell density state. Thirty genes were found to have >4-fold changes in expression (Figure 2A), and most (26/30) showed a decrease in expression in response to OHHL. Many of the OHHL-repressed genes have putative functions associated with insect pathogenesis. These include homologs of the PirAB insecticidal toxin (Sant_2443 and Sant_2444), genes encoding chitinases (Sant_1984 and Sant_1963), chitin-binding domain-containing proteins (Sant_1090 and Sant_P0292), and collagenase-like proteases (Sant_3444 and Sant_3445).

Only four genes demonstrated a significant increase in expression in response to OHHL. Curiously, the top two induced genes, *cpmA* and *cpmJ* (Sant_3163 and Sant_3164), were also induced in *S. glossinidius* and are homologous to components of the carbapenem biosynthesis gene cluster that is present in some enteric bacteria (Pontes et al., 2008). The other two genes induced by OHHL were a putative carbon starvation protein (*cstA*; Sant_2155) and a putative autoinducer 2 kinase (*lsrK*; Sant_3797) that may be involved in the regulation of another quorum-sensing pathway.

To determine the roles of YpeR and YenR in the regulation of expression via QS, we compared the RNA-seq profiles of Δ*ypeR* and Δ*yenR* mutant strains with the wild-type (WT) strain in the presence of OHHL (Figure 2A). Although both regulators clearly contribute to the differential regulation of the genes identified in the experiment involving the Δ*ypeI* mutant strain, the solo response regulator (YenR) has a more potent effect on differential regulation, given that the transcriptomic profile of the Δ*yenR* mutant strain more closely mimics that of a Δ*ypeI* mutant strain lacking OHHL. However, this seems to be due to the loss of OHHL synthase (YpeI) expression in the Δ*yenR* strain, which has ~50-fold less *ypeI* transcripts relative to the WT strain (Table S1; see entries highlighted in green on pages 2 and 3). To explore this further, we assayed the amount of OHHL produced by the WT, Δ*ypeI*, Δ*ypeR*, and Δ*yenR* strains. In liquid culture, the Δ*ypeI* strain failed to produce any OHHL (Figures 1B and 1C), consistent with the notion that *ypeI* is the only gene encoding an N-acyl HSL synthase in *S. praecaptivus*. This was further corroborated using an alternative reporter (*Chromobacterium violaceum* strain CV026; McClean et al., 1997), which also only detected a molecule produced by the WT strain (Figures 1D and 1E). In agreement with the transcriptomic data, the amount of OHHL produced by the Δ*yenR* mutant was greatly reduced relative to WT (~10-fold at 12 hr; Figure 1B), consistent with

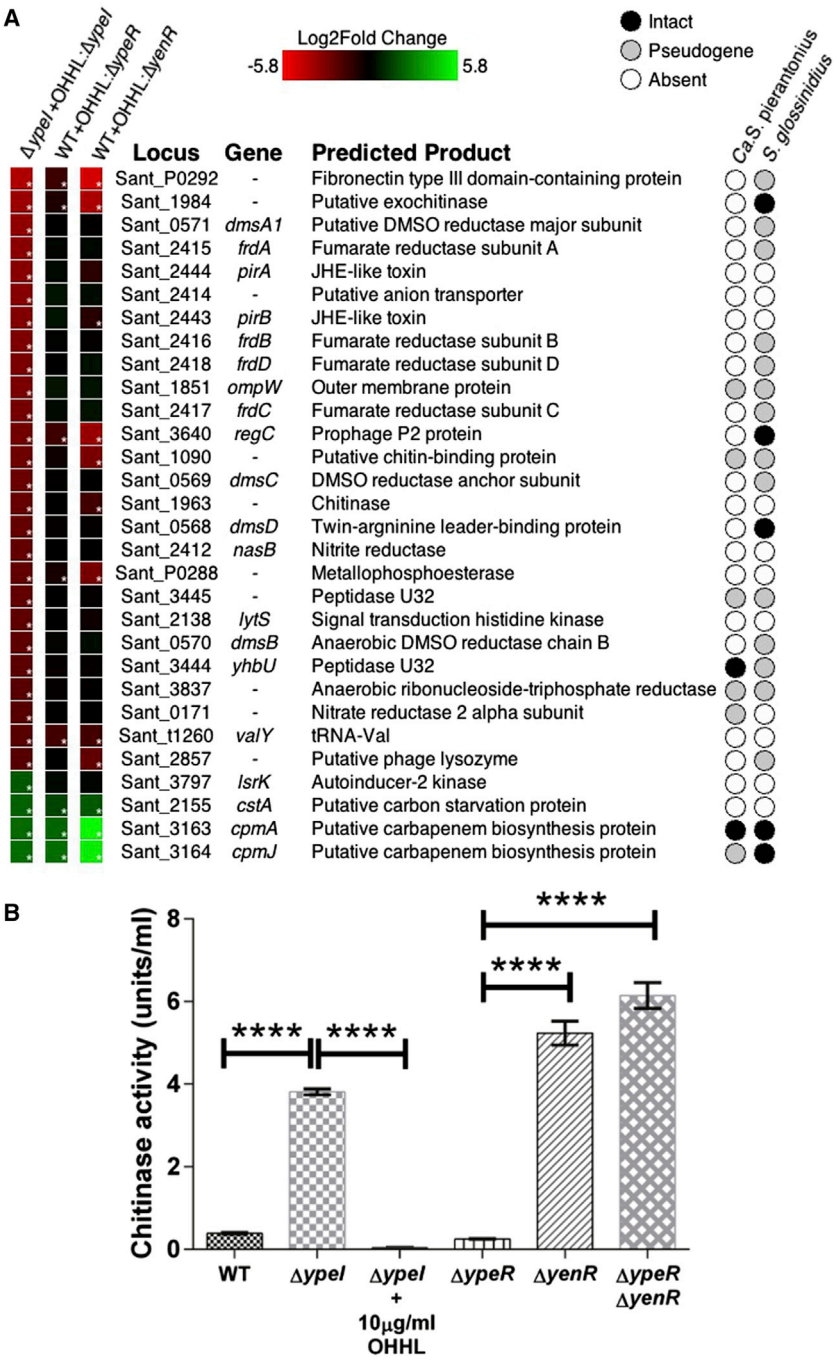

Figure 2. RNA-Seq Analysis of QS-Regulated Genes in *S. praecaptivus*

(A) Heatmaps showing changes in gene expression. The first column shows changes in the 30 most differentially expressed genes in the *S. praecaptivus* Δ*ypeI* strain in response to the addition of exogenous OHHL. The second and third columns show changes in the expression of the same 30 genes in a WT strain (supplemented with OHHL), relative to Δ*ypeR* and Δ*yenR* strains (respectively), lacking exogenous OHHL. The asterisks in the boxes on the left indicate statistically significant levels of differential expression. The matrix on the right reveals the status of the 30 genes in *Sodalis*-allied insect symbionts that are closely related to *S. praecaptivus*. Complete transcriptomic datasets are provided in Table S1.

(B) Chitinase activities of WT and mutant *S. praecaptivus* strains in the presence or absence of OHHL. All samples were assayed in triplicate, and error bars show standard deviations. One-way ANOVA comparisons between genotypes: Δ*ypeI* versus Δ*ypeI* supplemented with 10 μg/mL OHHL, WT versus Δ*ypeI*, Δ*ypeR* versus Δ*yenR*, and Δ*ypeR* versus Δ*ypeR*yenR* all yield ****$p < 0.0001$; Δ*yenR* versus Δ*ypeR* Δ*yenR* double mutant yields $p = 0.0006$.

absence of their signaling molecules, and their regulatory functions are antagonized by N-acyl homoserine lactones (AHLs) (Tsai and Winans, 2010). Genes encoding these particular *luxI* and *luxR* homologs (including those in *S. praecaptivus*) often overlap at their 3′ ends to mediate transcriptional antagonism. Taken together, these results indicate that there is a complex regulatory interplay between YpeI, YpeR, and YenR that facilitates QS-based signaling.

Validation of Transcriptomic Data

Since two *S. praecaptivus* genes encoding chitinases were significantly downregulated in response to OHHL, we performed chitinase assays in WT, Δ*ypeI*, Δ*ypeR*, and Δ*yenR* strains of *S. praecaptivus*. The highest activity was found in the Δ*ypeI* strain lacking OHHL (Figure 2B), consistent with the notion of QS-based repression. In addition, the Δ*ypeR* strain had a chitinase activity similar to the WT strain, indicating that YenR alone can repress chitinase in the presence of OHHL. Also, the Δ*yenR* mutant strain had significantly higher chitinase activity, consistent with the repression of OHHL synthesis. Together with the observation that the Δ*yenR* Δ*ypeR* double mutant has high chitinase activity, these results corroborate those obtained from RNA-seq analysis and the OHHL assays.

Quorum Sensing Suppresses Growth of *S. praecaptivus* In Vitro

During the course of our work, we noticed that the *S. praecaptivus* WT strain had a growth rate that was significantly

the notion that YenR enhances *ypeI* transcription and/or YpeR represses *ypeI* transcription. This is further supported by the fact that a Δ*yenR* Δ*yenR* double-mutant strain also produces a greatly reduced amount of OHHL and a Δ*ypeR* mutant strain shows an elevated level of OHHL production relative to WT (~10-fold at 12 hr; Figure 1B). However, the transcriptomic data show that the counts of *ypeI* transcripts are actually (~2-fold) lower in the Δ*ypeR* mutant relative to the WT strain, suggesting that the OHHL level in the culture media is also controlled by mechanisms other than the modulation of *ypeI* transcription. Interestingly, some LuxR homologs regulate transcription in the

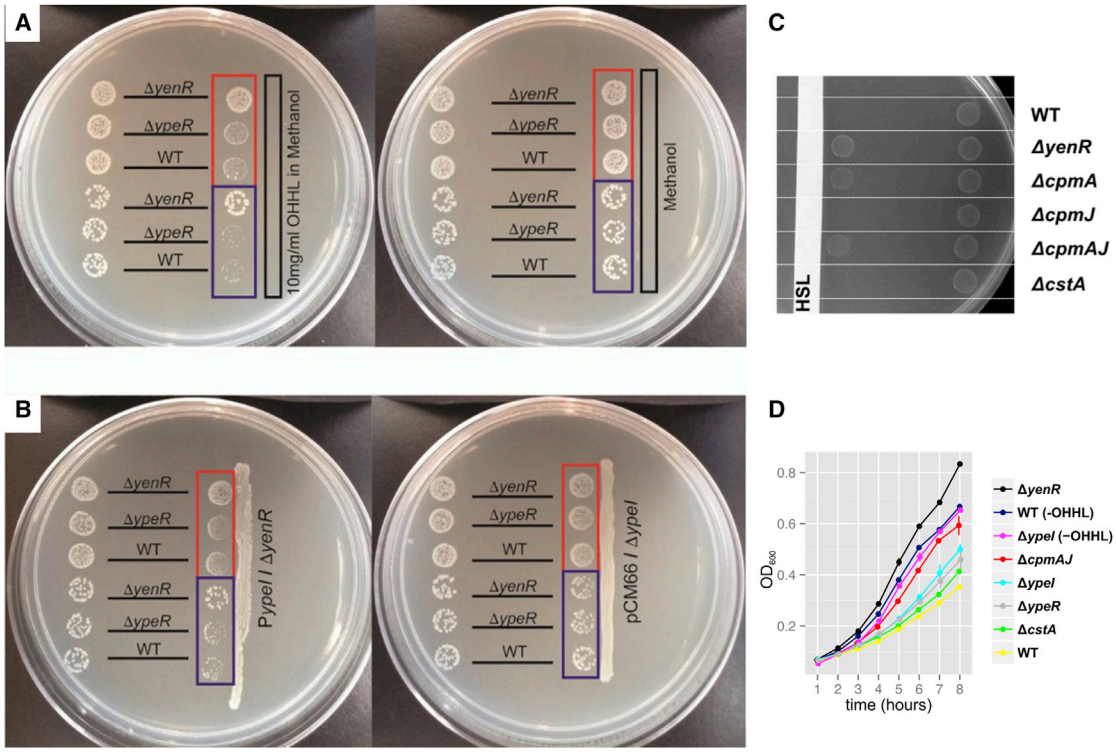

Figure 3. QS Induces Growth Suppression in *S. praecaptivus*

(A and B) Each bacterial strain (labeled according to genotype) was spotted in two positions on the plate. (A) shows spots placed either distal (left) or proximal (right) to a strip of sterile paper that was impregnated with exogenous OHHL in methanol (left plate) or methanol alone (right plate). (B) shows spots placed either distal (left) or proximal (right) to a streak of the *S. praecaptivus* Δ*yenR* strain maintaining plasmid pCM66 overexpressing the *ypeI* gene (left plate) or a streak of the *S. praecaptivus* Δ*ypeI* strain maintaining plasmid pCM66 lacking *ypeI* (right plate). The spots highlighted in the red boxes have a 10-fold higher concentration of cells than their counterparts highlighted in blue.

(C) *S. praecaptivus* strains (labeled according to genotype) were spotted in two positions on a plate, either proximal (left) or distal (right) to a strip of sterile paper impregnated with exogenous OHHL in methanol (labeled "HSL"). Note that deletion of *cpmA* alone relieves QS-mediated growth suppression. Deletion of either *cpmJ* or *cstA* (another gene whose transcription is increased under quorum) has no effect on growth rate.

(D) Assays of growth performed in liquid media containing 1 mg/mL OHHL or no OHHL as indicated by the "−OHHL" suffix. Data were obtained from three biological replicates, and error bars show standard errors. Note that growth is enhanced by deletion of *yenR* or *cpmAJ*.

reduced relative to the Δ*ypeI* mutant (Figure 1C). This was corroborated by a series of experiments performed on solid media, which show that OHHL inhibits growth of both the *S. praecaptivus* WT and the Δ*ypeR* mutant strains, but not the Δ*yenR* strain (Figure 3A). In addition, a plasmid overexpressing the OHHL synthase (YpeI) could only be maintained in a Δ*yenR* background, and this strain strongly inhibited the growth of adjacent WT and Δ*ypeR* (but not Δ*yenR*) strains (Figure 3B).

In order to identify the gene(s) responsible for this growth suppression in vitro, we generated mutant strains of *S. praecaptivus* lacking genes identified in the transcriptomic analysis (Table S1) and screened for relief of growth suppression. This led to the discovery that *cmpA* (but not the adjacent *cpmJ* gene) is largely responsible for the growth suppression phenotype observed in this study (Figures 3C and 3D). Curiously, while *cpmA* and *cpmJ* share significant sequence identity with components of an antibiotic (carbepenem) biosynthesis pathway found in other Gram-negative bacteria (Coulthurst et al., 2005; Derzelle et al., 2002), the majority of genes in this pathway are absent in *Sodalis* spp., and their CpmA homologs lack a critical region of a β-lactam synthase, indicating that they cannot make this antibiotic. Conservation of an asparagine synthase domain in CpmA suggests that its function involves amidohydrolase activity (Miller et al., 2003), which has wide-ranging functions in nature. Notably, the transcriptomic data (Table S1) show that *cpmA* is the 12th most abundant protein-coding transcript in the presence of OHHL, and since *cpmA* has been retained under the control of QS in two insect symbionts, (Pontes et al., 2008), we conclude that it likely has an important function in symbiotic interactions.

QS Controls a Weevil-Killing Phenotype

In order to examine the role of QS in vivo, we microinjected WT and mutant strains of *S. praecaptivus* into newly emerged adult grain weevils (*S. zeamais*), pre-treated to remove their native symbiont (SZPE), which is a very close relative of *S. praecaptivus* (Oakeson et al., 2014). The use of aposymbiotic weevils ensures that the results obtained in the current study only reflect the interaction between the weevil, *S. praecaptivus*, and its endogenous QS system. In addition, symbiont-free weevils are considerably easier to microinject because *Ca*. S. pierantonius provides the weevil with nutrients (aromatic amino acids) that harden the cuticle (Vigneron et al., 2014). Following microinjection, weevil mobility

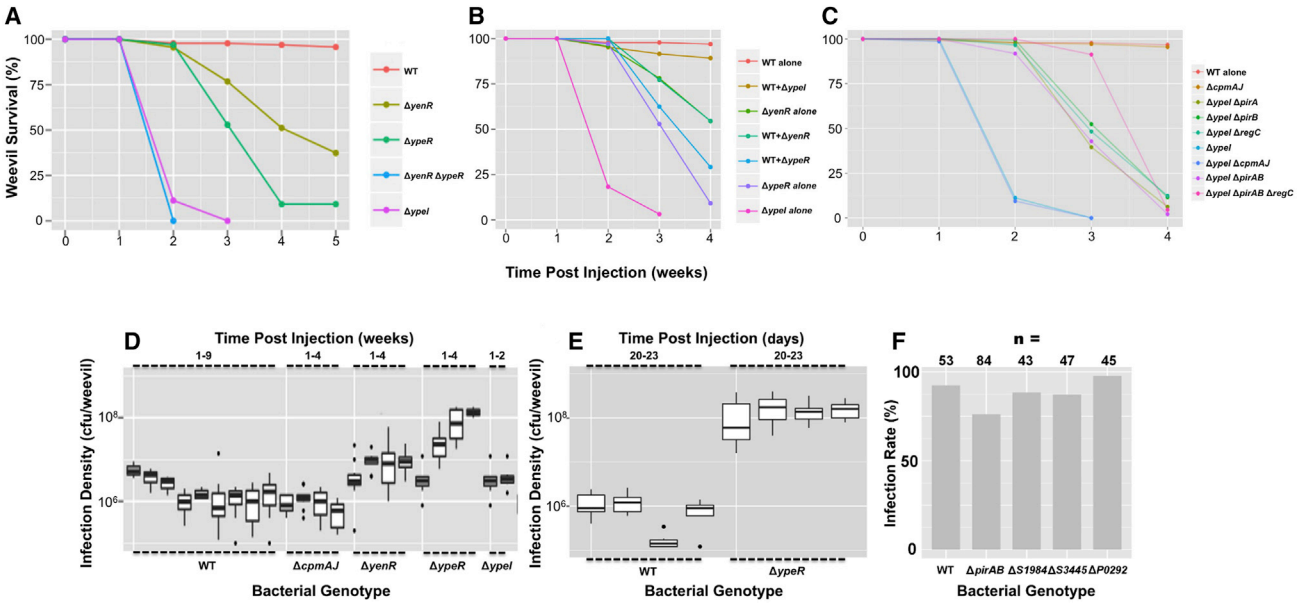

Figure 4. Weevil Survival Following Injection of WT and Mutant *S. praecaptivus*

(A) Inactivation of genes involved in the *S. praecaptivus* QS system results in weevil killing. Inactivation of both *ypeR* and *yenR* in a double-mutant strain yields the most potent killing phenotype.

(B) The WT strain complements the killing phenotype of the Δ*ypeI* mutant strain following co-injection. Note that the "+" symbol indicates injection of a 1:1 mixture of WT and respective mutant strain.

(C) Identification of genes that mediate weevil killing. Inactivation of *pirA*, *pirB*, and *regC* genes produce a significant delay in weevil killing in a Δ*ypeI* genetic background, with PirAB and RegC having a synergistic effect. Data and results of statistical tests related to (A)–(C) are reported in Tables S2 and S3.

(D and E) Bacterial infection densities are depicted as boxplots for a range of different *S. praecaptivus* strains at various time intervals following microinjection. Note that the infection densities of the Δ*yenR* and Δ*ypeR* strains increase over time relative to the WT and Δ*cpmAJ* strains (D), particularly in the latter stages of infection, concomitant with insect death (E).

(F) Weevil infection rates observed 7 days after injection of a reduced number of bacterial cells (1:10 dilution of overnight culture). Statistical analysis of the data (likelihood ratio test) shows that the Δ*pirAB* strain has a reduced infection rate relative to the other strains tested ($p = 0.0084$).

and survival were monitored daily (Figure S1; Table S2). At 1 week following injection, weevils injected with the Δ*ypeI* strain became lethargic (Figure S1) and died over the course of the next 2 weeks (Figure 4A). Weevils injected with the wild-type strain suffered no lethargy or death aside from a small percentage of early deaths resulting from injuries sustained as a consequence of microinjection (<5%).

Injection of the Δ*ypeR* and Δ*yenR* mutant strains yielded a delayed/reduced killing effect relative to the Δ*ypeI* strain, and a Δ*yenR* Δ*ypeR* double mutant killed as effectively and rapidly as the Δ*ypeI* mutant (Figure 4A). Further confirmation of the role of QS in killing was obtained by injection with a 1:1 mixture of WT and mutant strains. WT bacteria suppressed the killing effect of the Δ*ypeI* mutant by providing a source of exogenous OHHL (Figure 4B). However, WT bacteria did not mitigate the killing of the Δ*ypeR* or Δ*yenR* mutant strains because they lack the means to respond to OHHL. These results show that YpeR and YenR act synergistically to repress expression of genes involved in killing, with YpeR (Δ*yenR*) having a more potent effect. This contrasts with the in vitro results and suggests that the regulatory interactions between YenR, YpeR, and YpeI function in a different way in vivo likely as a consequence of distinct physical conditions or the influence of additional regulatory elements. Nonetheless, the results clearly show that strains of *S. praecaptivus* lacking any of the three genic components of the QS system have a potent weevil-killing phenotype that is suppressed in WT bacteria.

Identification of the Genic Effectors of Killing

In order to identify the QS-regulated genes that are responsible for weevil killing, we identified differentially expressed genes that might play a role in killing based on their predicted functions. These genes (highlighted in yellow in Table S2) were then knocked out in a Δ*ypeI* mutant background, and the resulting double mutants were injected into weevils to assess their killing capability. None of the double mutants tested were completely relieved of their weevil-killing phenotype. However, the Δ*ypeI* Δ*regC*, Δ*ypeI* Δ*pirA*, and Δ*ypeI* Δ*pirB* double-mutant strains all demonstrated a statistically significant delay in killing (Figure 4C; Tables S2 and S3). Comparative analysis of Δ*pirA*, Δ*pirB*, and Δ*pirAB* mutant strains yielded results that are consistent with the notion that PirA and PirB constitute a binary toxin complex, requiring both components for activity. The highest level of suppression was observed with a Δ*ypeI* Δ*pirAB* Δ*regC* quadruple mutant, suggesting that RegC and PirAB function independently to impact killing. However, even this strain was not completely suppressed in terms of killing.

We also tested the effect of a Δ*ypeI* Δ*sant_1962* double mutant, because this protein shares high sequence identity with insecticidal endotoxins and is also differentially regulated

by OHHL (adjusted p = 0.09; Table S1). However, weevils injected with this strain showed no suppression of killing relative to the Δ*ypeI* single mutant (Table S3). All other genes encoding putative toxins (Sant_0919, Sant_1053, and Sant_2840) displayed no significant reduction in expression in the presence of OHHL in the transcriptomic analyses (Table S1). Thus, we conclude that there are other effectors of killing or combinatorial effects that have not been identified in our limited screen.

In order to examine the role of CpmA-mediated growth suppression in killing, we also injected weevils with Δ*cpmAJ* mutant strains. However, deletion of *cpmAJ* had no effect on killing either when the mutation was maintained alone or in a Δ*ypeI* background (Figure 4C). Bacterial infection densities remained constant for the WT strain throughout the course of weevil infection, whereas the Δ*ypeR* and Δ*yenR* strains demonstrated a >10-fold and ~2-fold increase in infection density, respectively, consistent with their enhanced virulence properties (Figures 4D and 4E; Table S2). However, the Δ*cpmAJ* strain maintained lower numbers in the insect, especially at the onset of infection, consistent with the notion that CpmA has an adaptive role in vivo.

Loss of PirAB Impairs the Ability of *S. praecaptivus* to Infect Weevils

To determine whether the virulence factors identified in this study have an adaptive role during the initial stages of *S. praecaptivus* infection, we injected reduced numbers of WT and mutant strains of *S. praecaptivus* into weevils and screened for the presence of bacteria at 7 days post-infection. Only the Δ*pirAB* mutant strain was found to have a statistically significant infection defect (Figure 4F). It should be noted, however, that virulence is clearly a polygenic trait in *S. praecaptivus*, and many of the putative virulence factors identified in our transcriptomic screen have redundant functions (e.g., chitinases). In addition, microinjection is not a natural route of infection and might obviate the requirement for bacteria to utilize virulence factors to degrade the host integument.

DISCUSSION

In this study, we show that *S. praecaptivus* maintains a QS system with complex regulatory dynamics that utilizes the same signaling molecule (OHHL) and is genetically orthologous to the system previously characterized in the tsetse fly symbiont *S. glossinidius* (Pontes et al., 2008). However, transcriptomic analyses show that these bacteria differ markedly in the target genes that are regulated by QS. Indeed, the only component of QS-mediated regulation that is shared between *S. praecaptivus* and *S. glossinidius* involves upregulation of *cpmA* and *cpmJ* transcripts in response to OHHL. The work outlined here shows that CpmA mediates the suppression of *S. praecaptivus* growth in vitro in response to the QS signal OHHL. This OHHL-mediated growth suppression is eliminated in mutant strains lacking *cpmA*, *ypeI* (encoding the OHHL synthase), or *yenR* (a QS response regulator).

The transcriptomic analyses in this study show that the *S. praecaptivus* QS system has some unique properties that have been lost in *S. glossinidius* as a consequence of genome degeneration in the obligate insect-associated lifestyle (Clayton et al., 2012). Principal among these is the observation that QS reduces the expression of virulence factors that are anticipated to target insects, including insecticidal toxins and enzymes that degrade the insect integument. We compared the effects of injecting WT and QS mutant strains of *S. praecaptivus* into a weevil host. This led to the striking finding that QS-deficient strains have a potent weevil-killing phenotype. Thus, it appears that the QS system has evolved to maintain a benign and long-lasting infection in the weevil. Subsequent experiments revealed that killing is mediated by virulence factors rather than (CpmA-mediated) growth suppression.

The binary insecticidal Pir toxins were initially identified as key virulence factors in the insect pathogen *Photorhabdus luminescens* (Waterfield et al., 2005). They were subsequently found in other pathogenic bacteria, including *Vibrio parahaemolyticus*, in which they play an important role in shrimp pathogenesis (Sirikharin et al., 2015). It was shown that the crystal structure of the *V. parahaemolyticus* Pir toxin complex resembles those of the *Bacillus thuringiensis* Cry toxins, suggesting that they may have a conserved mode of action that ultimately causes destabilization of the host cell cytoskeleton, leading to cell death (Lee et al., 2015). Another gene identified to impact weevil killing by *S. praecaptivus* (*regC*) shares substantial sequence and structural homology with a bacteriophage P2 transcriptional repressor. It may serve as a secondary transcriptional regulator in the QS circuit, modulating the transcription of additional gene(s) that enhance the killing phenotype that were not identified in our limited screen. This is supported by the observation that the deletion of *pirAB* and *regC* has an additive effect in suppressing the killing mediated by the QS-defective Δ*ypeI* strain.

Since QS reduces the expression of genes (including *pirAB* and *regC*) under conditions of high bacterial population density, it stands to reason that these genes should provide a beneficial function when their expression is elevated at low bacterial population density. Since infections must commence from low density, the functions of these virulence genes are expected to be important in mediating entry of host tissues and cells. Consistent with this interpretation, the recently derived insect symbionts *S. glossinidius* and *Ca*. S. pierantonius have already lost many of the QS-regulated virulence genes, including *pirAB*. This is anticipated to occur as a consequence of the transition to permanent insect association because endosymbionts do not have to undertake cyclical infection of hosts. Furthermore, our results show that a mutant strain of *S. praecaptivus* lacking PirAB is deficient in its ability to establish infection in weevils via microinjection.

Notably, the attenuation of virulence (toward the vector) is predicted to be an important adaptation for a vector-borne pathogen because virulence decreases host fitness and therefore reduces the likelihood of successful (vector-borne) pathogen dispersal (Elliot et al., 2003; Ewald, 1987). It is also one of the two criteria, along with a switch from horizontal to vertical transmission, predicted to be of key importance in the evolutionary transition from parasitism to mutualism (Ewald, 1987). To this end, the QS system in *S. praecaptivus* acts to enhance the ability of this bacterium to maintain a long-standing infection in an insect host. This mechanism of gene expression control mitigates one side of the double-edged sword of virulence by limiting the harm inflicted upon the host once a successful infection has been established. At one level, this distinguishes *S. praecaptivus* from a wide variety of pathogenic bacteria, including the entomopathogen *Bacillus*

thuringiensis (Dubois et al.. 2012), that utilize QS to enhance the expression of virulence factors at high infection densities in order to facilitate a concerted and debilitating attack on the host (Winzer and Williams, 2001; Von Bodman et al., 2003; Antunes et al., 2010; Rutherford and Bassler; 2012; Papenfort and Bassler, 2016). At another level, it presents an interesting parallel to the pathoadaptive microniche evolution observed in chronic cystic fibrosis lung infections involving *Pseudomonas aeruginosa*, in which mutations accumulate in regulatory systems and genes responsible for the production of virulence factors that facilitate acute infection (Smith et al., 2006). This has been proposed to be adaptive because these particular virulence factors are predicted to be major drivers of inflammatory responses (Smith et al., 2006). However, it is also conceivable that such adaptations arise simply as a consequence of relaxed selection on the utility of these virulence factors following initiation of infection (Winstanley et al., 2016). Of course, since multiple null mutations cannot readily be reverted, the resulting strains are expected to be attenuated in terms of their capability to initiate de novo acute infections. Thus, one advantage of utilizing QS to control the activity of virulence factors, as highlighted in our study, is that regulatory control can be maintained over recurrent cycles of infection until a stable mutualistic association becomes established, and the virulence genes are then inactivated and lost in the process of genome degeneration.

STAR★METHODS

Detailed methods are provided in the online version of this paper and include the following:

- KEY RESOURCES TABLE
- CONTACT FOR REAGENT AND RESOURCE SHARING
- EXPERIMENTAL MODEL AND SUBJECT DETAILS
  - Insects
  - Bacteria
- METHOD DETAILS
  - Genetic Modification
  - OHHL Extraction and TLC Assay
  - OHHL Bioassays
  - Transcriptomics
  - Chitinase Assay
  - Growth Suppression Assays
  - Weevil Microinjection
  - Weevil Motility Assay
  - Bacterial Isolation from Weevils
- QUANTIFICATION AND STATISTICAL ANALYSIS
  - Transcriptomics
  - Statistical Analyses
- DATA AND SOFTWARE AVAILABILITY

SUPPLEMENTAL INFORMATION

Supplemental Information includes one figure and four tables and can be found with this article online at http://dx.doi.org/10.1016/j.chom.2017.04.003.

AUTHOR CONTRIBUTIONS

S.E. and C.D. designed experiments. S.E., A.L.C., and A.C. performed experiments. C.D., A.C., and S.E. wrote the paper.

ACKNOWLEDGMENTS

This work was supported by the National Institutes of Health (grant number 1R01AI095736 awarded to C.D.).

Received: November 23, 2016
Revised: February 15, 2017
Accepted: April 19, 2017
Published: May 10, 2017

REFERENCES

Anders, S., Pyl, P.T., and Huber, W. (2015). HTSeq—a Python framework to work with high-throughput sequencing data. Bioinformatics *31*, 166–169.

Antunes, L.C., Ferreira, R.B., Buckner, M.M., and Finlay, B.B. (2010). Quorum sensing in bacterial virulence. Microbiology *156*, 2271–2282.

Clayton, A.L., Oakeson, K.F., Gutin, M., Pontes, A., Dunn, D.M., von Niederhausern, A.C., Weiss, R.B., Fisher, M., and Dale, C. (2012). A novel human-infection-derived bacterium provides insights into the evolutionary origins of mutualistic insect-bacterial symbioses. PLoS Genet. *8*, e1002990.

Coulthurst, S.J., Barnard, A.M., and Salmond, G.P. (2005). Regulation and biosynthesis of carbapenem antibiotics in bacteria. Nat. Rev. Microbiol. *3*, 295–306.

Datsenko, K.A., and Wanner, B.L. (2000). One-step inactivation of chromosomal genes in Escherichia coli K-12 using PCR products. Proc. Natl. Acad. Sci. USA *97*, 6640–6645.

Derzelle, S., Duchaud, E., Kunst, F., Danchin, A., and Bertin, P. (2002). Identification, characterization, and regulation of a cluster of genes involved in carbapenem biosynthesis in Photorhabdus luminescens. Appl. Environ. Microbiol. *68*, 3780–3789.

Douglas, A.E. (2009). The microbial dimension in insect nutritional ecology. Funct. Ecol. *23*, 38–47.

Douglas, A.E. (2014). Symbiosis as a general principle in eukaryotic evolution. Cold Spring Harb. Perspect. Biol. *6*, a016113.

Dubois, T., Faegri, K., Perchat, S., Lemy, C., Buisson, C., Nielsen-LeRoux, C., Gohar, M., Jacques, P., Ramarao, N., Kolstø, A.B., and Lereclus, D. (2012). Necrotrophism is a quorum-sensing-regulated lifestyle in Bacillus thuringiensis. PLoS Pathog. *8*, e1002629.

Elliot, S.L., Adler, F.R., and Sabelis, M.W. (2003). How virulent should a parasite be to its vector? Ecology *84*, 2568–2574.

Ewald, P.W. (1987). Transmission modes and evolution of the parasitism-mutualism continuum. Ann. N Y Acad. Sci. *503*, 295–306.

Fuqua, C., Parsek, M.R., and Greenberg, E.P. (2001). Regulation of gene expression by cell-to-cell communication: acyl-homoserine lactone quorum sensing. Annu. Rev. Genet. *35*, 439–468.

Husnik, F., and McCutcheon, J.P. (2016). Repeated replacement of an intrabacterial symbiont in the tripartite nested mealybug symbiosis. Proc. Natl. Acad. Sci. USA *113*, E5416–E5424.

Kaiwa, N., Hosokawa, T., Kikuchi, Y., Nikoh, N., Meng, X.Y., Kimura, N., Ito, M., and Fukatsu, T. (2010). Primary gut symbiont and secondary, Sodalis-allied symbiont of the Scutellerid stinkbug Cantao ocellatus. Appl. Environ. Microbiol. *76*, 3486–3494.

Langmead, B., and Salzberg, S.L. (2012). Fast gapped-read alignment with Bowtie 2. Nat. Methods *9*, 357–359.

Lee, C.-T., Chen, I.-T., Yang, Y.-T., Ko, T.-P., Huang, Y.-T., Huang, J.-Y., Huang, M.-F., Lin, S.-J., Chen, C.-Y., Lin, S.-S., et al. (2015). The opportunistic marine pathogen Vibrio parahaemolyticus becomes virulent by acquiring a plasmid that expresses a deadly toxin. Proc. Natl. Acad. Sci. USA *112*, 10798–10803.

Lefèvre, C., Charles, H., Vallier, A., Delobel, B., Farrell, B., and Heddi, A. (2004). Endosymbiont phylogenesis in the dryophthoridae weevils: evidence for bacterial replacement. Mol. Biol. Evol. *21*, 965–973.

Love, M.I., Huber, W., and Anders, S. (2014). Moderated estimation of fold change and dispersion for RNA-seq data with DESeq2. Genome Biol. *15*, 550.

McClean, K.H., Winson, M.K., Fish, L., Taylor, A., Chhabra, S.R., Camara, M., Daykin, M., Lamb, J.H., Swift, S., Bycroft, B.W., et al. (1997). Quorum sensing and Chromobacterium violaceum: exploitation of violacein production and inhibition for the detection of N-acylhomoserine lactones. Microbiology *143*, 3703–3711.

Miller, M.T., Gerratana, B., Stapon, A., Townsend, C.A., and Rosenzweig, A.C. (2003). Crystal structure of carbapenam synthetase (CarA). J. Biol. Chem. *278*, 40996–41002.

Moran, N.A., McCutcheon, J.P., and Nakabachi, A. (2008). Genomics and evolution of heritable bacterial symbionts. Annu. Rev. Genet. *42*, 165–190.

Nadarasah, G., and Stavrinides, J. (2011). Insects as alternative hosts for phytopathogenic bacteria. FEMS Microbiol. Rev. *35*, 555–575.

Oakeson, K.F., Gil, R., Clayton, A.L., Dunn, D.M., von Niederhausern, A.C., Hamil, C., Aoyagi, A., Duval, B., Baca, A., Silva, F.J., et al. (2014). Genome degeneration and adaptation in a nascent stage of symbiosis. Genome Biol. Evol. *6*, 76–93.

Oliver, K.M., Degnan, P.H., Burke, G.R., and Moran, N.A. (2010). Facultative symbionts in aphids and the horizontal transfer of ecologically important traits. Annu. Rev. Entomol. *55*, 247–266.

Papenfort, K., and Bassler, B.L. (2016). Quorum sensing signal-response systems in Gram-negative bacteria. Nat. Rev. Microbiol. *14*, 576–588.

Pontes, M.H., Babst, M., Lochhead, R., Oakeson, K., Smith, K., and Dale, C. (2008). Quorum sensing primes the oxidative stress response in the insect endosymbiont, Sodalis glossinidius. PLoS One *3*, e3541.

Rutherford, S.T., and Bassler, B.L. (2012). Bacterial quorum sensing: its role in virulence and possibilities for its control. Cold Spring Harb. Perspect. Med. *2*, a012427.

Sachs, J.L., Skophammer, R.G., Bansal, N., and Stajich, J.E. (2013). Evolutionary origins and diversification of proteobacterial mutualists. Proc. Biol. Sci. *281*, 20132146, http://dx.doi.org/10.1098/rspb.2013.2146.

Sirikharin, R., Taengchaiyaphum, S., Sanguanrut, P., Chi, T.D., Mavichak, R., Proespraiwong, P., Nuangsaeng, B., Thitamadee, S., Flegel, T.W., and Sritunyalucksana, K. (2015). Characterization and PCR detection of binary, Pir-like toxins from Vibrio parahaemolyticus isolates that cause acute hepatopancreatic necrosis disease (AHPND) in shrimp. PLoS One *10*, e0126987.

Smith, E.E., Buckley, D.G., Wu, Z., Saenphimmachak, C., Hoffman, L.R., D'Argenio, D.A., Miller, S.I., Ramsey, B.W., Speert, D.P., Moskowitz, S.M., et al. (2006). Genetic adaptation by Pseudomonas aeruginosa to the airways of cystic fibrosis patients. Proc. Natl. Acad. Sci. USA *103*, 8487–8492.

Snyder, A.K., McMillen, C.M., Wallenhorst, P., and Rio, R.V. (2011). The phylogeny of Sodalis-like symbionts as reconstructed using surface-encoding loci. FEMS Microbiol. Lett. *317*, 143–151.

Toju, H., and Fukatsu, T. (2011). Diversity and infection prevalence of endosymbionts in natural populations of the chestnut weevil: relevance of local climate and host plants. Mol. Ecol. *20*, 853–868.

Tsai, C.S., and Winans, S.C. (2010). LuxR-type quorum-sensing regulators that are detached from common scents. Mol. Microbiol. *77*, 1072–1082.

Vallet-Gely, I., Lemaitre, B., and Boccard, F. (2008). Bacterial strategies to overcome insect defences. Nat. Rev. Microbiol. *6*, 302–313.

Vigneron, A., Masson, F., Vallier, A., Balmand, S., Rey, M., Vincent-Monégat, C., Aksoy, E., Aubailly-Giraud, E., Zaidman-Rémy, A., and Heddi, A. (2014). Insects recycle endosymbionts when the benefit is over. Curr. Biol. *24*, 2267–2273.

Von Bodman, S.B., Bauer, W.D., and Coplin, D.L. (2003). Quorum sensing in plant-pathogenic bacteria. Annu. Rev. Phytopathol. *41*, 455–482.

Waterfield, N., Kamita, S.G., Hammock, B.D., and ffrench-Constant, R. (2005). The Photorhabdus Pir toxins are similar to a developmentally regulated insect protein but show no juvenile hormone esterase activity. FEMS Microbiol. Lett. *245*, 47–52.

Waters, C.M., and Bassler, B.L. (2005). Quorum sensing: cell-to-cell communication in bacteria. Annu. Rev. Cell Dev. Biol. *21*, 319–346.

Winstanley, C., O'Brien, S., and Brockhurst, M.A. (2016). Pseudomonas aeruginosa evolutionary adaptation and diversification in cystic fibrosis chronic lung infections. Trends Microbiol. *24*, 327–337.

Winzer, K., and Williams, P. (2001). Quorum sensing and the regulation of virulence gene expression in pathogenic bacteria. Int. J. Med. Microbiol. *291*, 131–143.

Zhu, J., Chai, Y., Zhong, Z., Li, S., and Winans, S.C. (2003). Agrobacterium bioassay strain for ultrasensitive detection of N-acylhomoserine lactone-type quorum-sensing molecules: detection of autoinducers in Mesorhizobium huakuii. Appl. Environ. Microbiol. *69*, 6949–6953.

STAR★METHODS

KEY RESOURCES TABLE

REAGENT or RESOURCE	SOURCE	IDENTIFIER
Bacterial and Virus Strains		
Sodalis praecaptivus wild-type	ATCC	BAA-2554
Sodalis praecaptivus ΔypeI::Kan	This study	CD3
Sodalis praecaptivus ΔypeI::Spc	This study	CD298
Sodalis praecaptivus ΔypeR::Spc	This study	CD286
Sodalis praecaptivus ΔyenR::Spc	This study	CD384
Sodalis praecaptivus ΔypeR::Gen ΔyenR::Spc	This study	CD433
Sodalis praecaptivus ΔypeI::Spc Δ(agaR–agaF)::Gen	This study	CD302
Sodalis praecaptivus Δ(agaR–agaF)::Gen	This study	CD269
Sodalis praecaptivus ΔypeI::Spc ΔpirA::Gen	This study	CD395
Sodalis praecaptivus ΔpirA::Gen	This study	CD334
Sodalis praecaptivus ΔypeI::Spc ΔpirB::Gen	This study	CD314
Sodalis praecaptivus ΔpirB::Gen	This study	CD317
Sodalis praecaptivus ΔypeI::Spc ΔpirAB::Gen	This study	CD326
Sodalis praecaptivus ΔpirAB::Gen	This study	CD330
Sodalis praecaptivus ΔypeI::Spc Δsant_1963::Gen	This study	CD321
Sodalis praecaptivus Δsant_1963::Gen	This study	CD265
Sodalis praecaptivus ΔypeI::Spc Δsant_1090::Gen	This study	CD322
Sodalis praecaptivus Δsant_1090::Gen	This study	CD323
Sodalis praecaptivus ΔypeI::Spc Δsant_2430::Gen	This study	CD338
Sodalis praecaptivus Δsant_2430::Gen	This study	CD336
Sodalis praecaptivus ΔypeI::Spc ΔcpmAJ::Gen	This study	CD348
Sodalis praecaptivus ΔcpmAJ::Gen	This study	CD345
Sodalis praecaptivus ΔcpmA::Gen	This study	CD533
Sodalis praecaptivus ΔcpmJ::Gen	This study	CD549
Sodalis praecaptivus ΔypeI::Spc Δsant_1984::Gen	This study	CD351
Sodalis praecaptivus Δsant_1984::Gen	This study	CD354
Sodalis praecaptivus ΔypeI::Spc Δsant_1984::Kan Δsant_1963::Gen	This study	CD440
Sodalis praecaptivus Δsant_1984::Gen Δsant_1963::Kan	This study	CD560
Sodalis praecaptivus ΔypeI::Spc ΔregC::Gen	This study	CD361
Sodalis praecaptivus ΔregC::Gen	This study	CD358
Sodalis praecaptivus ΔypeI::Spc ΔregC::Kan ΔpirAB::Gen	This study	CD857
Sodalis praecaptivus ΔypeI::Spc Δsant_P0288::Gen	This study	CD362
Sodalis praecaptivus Δsant_P0288::Gen	This study	CD365
Sodalis praecaptivus ΔypeI::Spc Δ(dmsA1–dmsD)::Gen	This study	CD376
Sodalis praecaptivus Δ(dmsA1–dmsD)::Gen	This study	CD372
Sodalis praecaptivus ΔypeI::Spc Δsant_2857::Gen	This study	CD398
Sodalis praecaptivus Δsant_2857::Gen	This study	CD367
Sodalis praecaptivus ΔypeI::Spc Δsant_P0292::Gen	This study	CD416
Sodalis praecaptivus Δsant_P0292::Gen	This study	CD339
Sodalis praecaptivus ΔcstA::Gen	This study	CD1191
Sodalis praecaptivus ΔypeI::Spc Δsant_1962::Gen	This study	CD1201

(*Continued on next page*)

Continued		
REAGENT or RESOURCE	SOURCE	IDENTIFIER
Sodalis praecaptivus ΔyenR::Spc (pCM66)	This study	CD478
Sodalis praecaptivus ΔyenR::Spc (pCM66–YpeI)	This study	CD476
Agrobacterium tumefaciens strain, KYC55 (pJZ372)(pJZ384)(pJZ410)	Zhu et al., 2003	N/A
Chromobacterium violaceum strain CV026	McClean et al., 1997	N/A
Sodalis glossinidius wild-type	Pontes et al., 2008	N/A
Chemicals, Peptides, and Recombinant Proteins		
OHHL	Sigma-Aldrich	K3255
Phusion High-Fidelity DNA Polymerase	Thermo Fisher Scientific	F530S
Mitsuhashi Maramorosch (MM) Medium	ABMgood	TM033
Taq Polymerase Mastermix	Thermo Fisher Scientific	K0171
AMPure XP beads	Agencourt	A63880
Critical Commercial Assays		
Chitinase assay	Sigma-Aldrich	CS1030
Purelink RNA minikit	Ambion	12183018A
TruSeq RNA library preparation kit	Illumina	RS-122-2001
Deposited Data		
RNA-seq data	This study	GEO: GSE97720
Experimental Models: Organisms/Strains		
Sitophilus zeamais	USDA, Manhattan, KS	N/A
Oligonucleotides		
See Table S3	N/A	N/A
Recombinant DNA		
Plasmid pCM66	This study	N/A
Plasmid pRed/Gamm (CAT)	Datsenko and Wanner, 2000	N/A
Plasmid pCM66-YpeI	This study	N/A
Software and Algorithms		
Bowtie2	Langmead and Salzberg, 2012	http://bowtie-bio.sourceforge.net/bowtie2/index.shtml; RRID: SCR_005476
DESeq2	Love et al., 2014	https://bioconductor.org/packages/release/bioc/html/DESeq2.html
R	N/A	https://www.r-project.org; RRID: SCR_001905
Processing	N/A	https://processing.org/
HTSeq	Anders et al., 2015	http://www-huber.embl.de/HTSeq/doc/overview.html; RRID: SCR_005514

CONTACT FOR REAGENT AND RESOURCE SHARING

Further information and requests for resources and reagents should be directed to and will be fulfilled by the Lead Contact, Colin Dale (colin.dale@utah.edu).

EXPERIMENTAL MODEL AND SUBJECT DETAILS

Insects

Sitophilus zeamais weevils (derived from a colony maintained by USDA, Manhattan, KS, U.S.A) were reared on organic whole yellow maize (Purcell Mountain Farms) in an incubator at 27°C and 60% relative humidity. Symbiont-free (aposymbiotic) weevils were generated by rearing on rifampicin treated corn prepared by hydrating dried corn with a 3% (w/v) solution of rifampicin (1 mg/ml), prior to addition of insects. After three generations on this antibiotic supplemented diet, loss of symbionts was confirmed by microscopic examination of 100 larvae (revealing absence of bacteriomes) and by negative PCR assays on whole weevil DNA using Taq Polymerase MasterMix (Thermo Fisher Scientific) using symbiont specific primers (1675 and 1676 in Table S4), with 35 cycles of PCR (95°C

15 s, 60°C, 30 s, 72°C 30 s). Aposymbiotic insects were subsequently maintained on a normal diet and checked periodically to confirm the absence of bacteriomes. Newly emerged adult weevils were assigned to experimental treatments groups randomly with respect to sex.

Bacteria

All experiments in the manuscript were conducted using the type strain of *S. praecaptivus* described in Clayton et al. (2012) and deposited at the American Type Culture Collection (ATCC) as product BAA-2554. All genetic mutants of *S. praecaptivus* described in this study were derived from this strain and cultured in LB media with appropriate antibiotics, at 30°C, unless otherwise described. *S. glossinidius* was cultured in MM medium at 25°C. AHL bioassays were conducted using two bacterial reporter strains: *A. tumefaciens* strain, KYC55 (Zhu et al., 2003) (pJZ372)(pJZ384)(pJZ410), was cultured in AT medium at 30°C and *Chromobacterium violaceum* strain CV026 (McClean et al., 1997) was cultured on LB agar at 30°C.

METHOD DETAILS

Genetic Modification

Gene disruptions/deletions in *S. praecaptivus* were achieved using the lambda Red recombineering procedure, as described previously (Datsenko and Wanner, 2000). Constructs were obtained using three step PCR reactions, as follows: Approximately 150 nucleotides of the 5′ and the 3′ of target genes were amplified by PCR with Phusion High Fidelity DNA Polymerase (Thermo Fisher Scientific) using the oligonucleotides and annealing temperatures listed in Table S4. Identical PCR conditions were employed for all construction steps unless otherwise indicated. For example, to disrupt *ypeI* with a Spectinomycin resistance cassette (Δ*ypeI*::Spc), primer pairs 232/233 and 234/235 were used. The PCR was performed for 35 cycles (98°C 5 s, 62°C, 30 s, 72°C 20 s) in identical reactions with and without 5% DMSO. The resulting PCR products were then purified with Agencourt AMPure XP beads (Beckman Coulter). The 5′ and 3′ flanking sequences were joined to antibiotic resistance cassettes cassettes (KanR, SpcR, or GenR) using Taq Polymerase MasterMix (Thermo Fisher Scientific), using the oligonucleotides and annealing temperatures listed in Table S4, in two steps. The first joining step was performed with only the three dsDNA template fragments in 10 cycles of PCR (95°C 15 s, 45°C, 30 s, 72°C 60 s) to facilitate hybridization. The second assembly step was performed with primer pairs as indicated in Table S4. For example, to create Δ*ypeI*::Spc, primer pairs 232/235 were used in a 35 cycle reaction (95°C 15 s, 58°C, 30 s, 72°C 60 s). The PCR products were again purified with Agencourt AMPure XP beads. The resulting dsDNA fragments were electroporated into an *S. praecaptivus* strain harboring the lambda Red-Gamm plasmid, pRed/Gamm (CAT). For transformation, *S. praecaptivus* cultures were grown in 25 mL 2YT5.8 media (20 g/l Tryptone, 8 g/l Yeast Extract, 10 g/l NaCl, adjusted to pH 5.8) until OD_{600} reached ~0.4 units. Expression of lambda Red-Gamm proteins was then induced by addition of 0.4% arabinose for 30 min. Cells were harvested and washed twice in ice-cold sterile water. DNA was electroporated into cells using an Eppendorf electroporator model 2510, at 1600 V/s. Following a six-hour recovery in LB medium, recombinant clones were then selected by plating on LB agar with the appropriate antibiotic(s). Gene disruptions were verified by PCR with Taq Polymerase MasterMix (Thermo Fisher Scientific) with primers pairs and annealing temperatures listed in Table S4. For example Δ*ypeI*::Spc was verified with primer pairs 236/138 and 237/139 in a 35 cycle reaction (95°C 15 s, 58°C, 30 s, 72°C 30 s). The resulting PCR products were purified using Agencourt AMPure XP beads and sequenced using the Sanger method to confirm the integrity of junctions between the antibiotic resistance marker and the bacterial chromosome.

OHHL Extraction and TLC Assay

OHHL extraction was performed on cultures of *S. glossinidius* (grown in liquid MM medium) and *S. praecaptivus* (grown in LB medium) were pelleted by centrifugation (8,000 g, 20 min., 4°C) once their turbidities reached an $O.D_{600}$ of ~0.4 units. The resulting culture supernatants were filtered through 0.22 micron pore-size membrane filters (Argos Technologies) and then extracted by shaking with an equal volume of ethyl acetate for 30 min. The ethyl acetate extracts were dried with anhydrous magnesium sulfate and filtered. The solvent was then evaporated using a vacuum centrifuge at 60°C and the OHHL-containing residue was resuspended in 100 μL methanol. These extracts were then subjected to TLC on a C_{18} reverse-phase plate (Whatman) using methanol:water (60:40) as the solvent/carrier. Following development, the plate was dried and overlaid with a live culture of *A. tumefaciens* strain KYC55 (pJZ372; pJZ384; pJZ410) (Zhu et al., 2003). For the *C. violaceum* AHL reporter assay, strain CV026 was streaked alongside *S. praecaptivus* on LB agar and incubated at 30°C for 48 hr.

OHHL Bioassays

The *S. praecaptivus* strains were cultured overnight in 4.5 mL LB liquid media. Bacteria from these cultures were pelleted, washed twice in 25 mL LB and resuspended in 20 mL fresh media to yield OD_{600} of 0.025 units. During a 12 hr incubation with shaking at 200 rpm and 30°C, the cultures were sampled every two hours to determine cell densities and to assay for the presence of OHHL with the β-galactosidase activity assay using an *A. tumefaciens* acyl-HSL reporter strain, as described previously (Zhu et al., 2003). Specifically, the culture was cleared of cells by centrifugation at 16,000 x g for 2 min. 20 μl of 10-fold serial dilutions of the supernatant were added to 180 μl of the preinduced reporter strain and incubated at 30°C for 16 hr without shaking. The β-galactosidase assays were performed on 100 μl of the reporter cell cultures. To estimate the concentration of OHHL in WT *S. praecaptivus*

culture media at OD_{600} of 0.4, OHHL extraction was performed from total culture supernatant into 200 μL of methanol, which was then used as substrate in the *A. tumefaciens* β-galactosidase assay. Solutions of 50, 500 and 1250 nM OHHL (Sigma Aldrich, K3255) were prepared in methanol for use as standards. The concentration of OHHL in the OD_{600} = 0.4 culture was determined to be ~1 μg OHHL/ml.

Transcriptomics

For transcriptomics, triplicate (biological replicate) 20 mL cultures of *S. praecaptivus* were grown in LB media, at 200 rpm shaking and 30°C, with or without supplementation with OHHL (10 μg/ml). Total nucleic acid was extracted from each culture using Triton X-100, following four hours of exposure (or lack of exposure) to OHHL for the comparison involving the Δ*ypeI* strain, or after five hours of growth for the comparisons involving the WT strain (supplemented with OHHL) and the Δ*ypeR* and Δ*yenR* strains. RNA was then purified using the Purelink RNA minikit (Ambion). The resulting RNA was then analyzed using an Agilent bioanalyzer to ensure that it lacked DNA contamination and was of sufficient quality for cDNA preparation. Sequencing libraries were prepared using the Illumina TruSeq method and sequencing on a HiSeq instrument (Illumina). The resulting quality fitered 50-base single reads were mapped to the reference genome using bowtie2 (Langmead and Salzberg, 2012) employing the–very-sensitive preset. Read counts mapping to individual genes were generating using HTSeq (Anders et al., 2015) by running htseq-count using the options -s no -a 0 -m intersection-nonempty -t gene. Next, using custom Perl scripts, counts from three biological replicate cultures were combined and subject to statistical analysis. After normalization, the combined counts files were compared using DESeq2 (Love et al., 2014).

Chitinase Assay

Chitinase activities in the *S. praecaptivus* culture supernatants were measured using a fluorimetric assay (Sigma-Aldrich, CS1030) according to the manufacturer's instructions. Cells were grown in LB media (15 mL volume), from a starting OD_{600} of 0.05, with 200 rpm shaking at 30°C until $O.D_{600}$ reached ~1 unit. 10 μL of culture supernatant was added to 90 μL of the substrate working solution (containing 4-methylumbelliferyl β-D-N, N-diacetylchitobioside hydrate) in a 96-well fluorescence plate (Greiner Bio-One, 655096) and incubated for 60 min at 37°C in the dark. The reaction was stopped by adding 200 μL of sodium carbonate buffer, and the fluorescence was measured with a SynergyMx plate reader (BioTek Instruments) within 15 min of the reaction end point. The chitinase activity was calculated using a 4-methyl umbelliferone standard.

Growth Suppression Assays

Plate growth assays were performed by spotting appropriate dilutions of overnight cultures on LB agar plates (lacking NaCl to inhibit swarming motility). OHHL was dissolved in methanol and added to sterile paper strips or pipetted directly onto plates. One recombinant *S. praecaptivus* strain, maintaining a pCM66 plasmid expressing *ypeI* in a Δ*yenR* background, overproduces OHHL without undergoing growth suppression and was also used as a source of OHHL by streaking it onto plates. A control strain was also utilized that maintains an empty pCM66 plasmid in a Δ*ypeI* background and therefore does not produce any OHHL. All plates were maintained at 30°C and observed for growth at daily intervals. Liquid assays were performed by maintaining triplicate cultures of WT and mutant strains of *S. praecaptivus* in LB media at 30°C with shaking at 200 rpm in the presence of 1 mg/ml OHHL and recording turbidity (OD_{600nm}) at hourly intervals

Weevil Microinjection

Newly emerged adult aposymbiotic weevils were microinjected with capillary tubes (3.5″ Drummond # 3-000-203-G/X, Drummond Scientific Company) that were pulled to create a short sharp tip (Bee-Stinger needle) with Micropipette puller P-97 (Sutter Instruments). The settings on the micropipette puller were as follows: Heat = 292, Pull = 100, Velocity = 60, Time = 250, Pressure = 500. Weevils were immobilized by a brief incubation on ice and the needle was immersed in 50 μl of overnight bacterial culture to collect bacteria by capillary action. The needle was then used to pierce the weevil in the thoracic region between the middle and hind legs. This resulted in a median 2800 bacterial cells being transferred into each weevil, as determined by plating weevil homogenates directly after injection. Following injection, weevils were then transferred to hydrated maize grains and maintained in an incubator at 27°C and 60% relative humidity.

Weevil Motility Assay

Individual weevils were placed in the center of an empty petri dish and the time taken for them to move from the center of the dish to the periphery was recorded. Weevils that displayed no sign of movement during the assay were excluded.

Bacterial Isolation from Weevils

Surface contaminants were removed from weevils by immersing the adult insects in a solution of 10% bleach for 5 min with agitation. Weevils were then air-dried and homogenized in 100 μl of sterile water. A bacterial dilution series was plated on LB agar (without NaCl) containing 50 μg/ml polymyxin B to select for *S. praecaptivus*.

QUANTIFICATION AND STATISTICAL ANALYSIS

Transcriptomics

RNA-Seq experiments were carried out in triplicate using independent bacterial cultures. Complete datasets derived from DESeq2-based analysis of RNaseq data are presented in Table S1.

Statistical Analyses

All statistical analyses were performed using the R software package. Data from chitinase assays were analyzed by ordinary one-way ANOVA comparisons. The numbers of insects used in the weevil microinjection experiments are reported in Table S2, along with their median lifespan. Pairwise log-rank tests were performed to compare lifespan of weevils injected with different strains of *S. praecaptivus* using the data summarized in Table S2. The results of these statistical analyses are presented in Table S3. The box and whisker plots presented in Figures 4D and 4E were obtained using the geom_boxplot function in R using the ggplot2 package. Statistical analysis of data relating to weevil infection at 7 days post microinjection (Figure 4F) was performed using a likelihood ratio test under the log-linear model in R. The numbers of insects sampled for this analysis are presented at the top of the figure panel. The numbers of insects sampled for bacterial quantification (Figure 4D; for data presented from left to right) were 10, 10, 10, 10, 10, 10, 10, 10, 12, 10, 10, 10, 12, 12, 12, 12, 9, 10, 10, 10, 2, 10, 9. For Figure 4E (left to right) the numbers were 8, 8, 8, 8, 7, 6, 8, 5.

DATA AND SOFTWARE AVAILABILITY

The accession number for the transcriptomics data reported in this paper is GEO: GSE97720.